IEEE Journal of Translational Engineering in Health and Medicine

Received 7 November 2017; revised 5 January 2018 and 14 February 2018; accepted 27 February 2018.
Date of publication 3 April 2018; date of current version 18 April 2018.

Digital Object Identifier 10.1109/JTEHM.2018.2815539

Toward Non-Invasive and Automatic Intravenous Infiltration Detection: Evaluation of Bioimpedance and Skin Strain in a Pig Model

A. OZAN BICEN[1], (Member, IEEE), LEANNE L. WEST[2], LILIANA CESAR[3], AND OMER T. INAN[1], (Senior Member, IEEE)

[1]Inan Research Laboratory, School of Electrical and Computer Engineering, Georgia Institute of Technology, Atlanta, GA 30332, USA
[2]Pediatric Technology Center, Georgia Institute of Technology, Atlanta, GA 30332, USA
[3]Independent Contributor, Atlanta, GA 30313, USA

CORRESPONDING AUTHOR: A. OZAN BICEN (bozan@ece.gatech.edu)

This work was supported by the Georgia Tech/Emory University Coulter Translational Research Partnership Program and the Pediatric Technology Center at Georgia Tech.

ABSTRACT Intravenous (IV) therapy is prevalent in hospital settings, where fluids are typically delivered with an IV into a peripheral vein of the patient. IV infiltration is the inadvertent delivery of fluids into the extravascular space rather than into the vein (and requires urgent treatment to avoid scarring and severe tissue damage), for which medical staff currently needs to check patients periodically. In this paper, the performance of two non-invasive sensing modalities, electrical bioimpedance (EBI), and skin strain sensing, for the automatic detection of IV infiltration was investigated in an animal model. Infiltrations were physically simulated on the hind limb of anesthetized pigs, where the sensors for EBI and skin strain sensing were co-located. The obtained data were used to examine the ability to distinguish between infusion into the vein and an infiltration event using bioresistance and bioreactance (derived from EBI), as well as skin strain. Skin strain and bioresistance sensing could achieve detection rates greater than 0.9 for infiltration fluid volumes of 2 and 10 mL, respectively, for a given false positive, i.e., false alarm rate of 0.05. Furthermore, the fusion of multiple sensing modalities could achieve a detection rate of 0.97 with a false alarm rate of 0.096 for 5mL fluid volume of infiltration. EBI and skin strain sensing can enable non-invasive and real-time IV infiltration detection systems. Fusion of multiple sensing modalities can help to detect expanded range of leaking fluid volumes. The provided performance results and comparisons in this paper are an important step towards clinical translation of sensing technologies for detecting IV infiltration.

INDEX TERMS Bioimpedance, detection performance, extravasation, IV infiltration, non-invasive sensing, sensor fusion, skin strain.

I. INTRODUCTION

Intravenous (IV) therapy enables fluid administration directly into the peripheral veins for delivery of medications and nutrients, as well as blood transfusion. IV infiltration (as well as extravasation) is the unintended leakage of fluid out of the targeted vein into the extravascular space (surrounding tissue and interstitial space), and is considered a medical emergency. Infiltration occurs as a result of a combination of factors, including solute concentration, infusion pressure, anatomical variability, and punctured lining of the vein [1]. The effects can be devastating, which include swelling, blistering, pain, and even tissue necrosis. Resulting injuries are considered to be medical emergencies and require immediate treatment [1]–[3].

Policies and procedures to prevent IV infiltration include strict protocols for IV administration to ensure secure catheter placement, frequently checking the IV site for early signs of infiltration, and monitoring of infusion pump pressures and volumes [4]. In the case that the caregiver does not have a clear line of sight to the IV catheter site, or the

patient is unable to communicate with the medical staff, an IV infiltration may not be noticed in a timely manner. This is often the case when the patient is under anesthesia and having surgery with the IV catheter site draped [5]. Detecting IV infiltration among infants and children is also rather challenging, since infants and children have difficulty communicating the pain or discomfort to the nursing staff. Thus, unfortunately, approximately 4% of infants receiving IV therapy in neonatal intensive care units are exposed to cosmetically or functionally significant scars connected to IV infiltration injuries [3], [6]. While there are treatments that can alleviate these side effects, non-invasive and early detection of IV infiltration with minimum number of false alarms would have substantial impact on patient safety for children and adults receiving IV therapy.

Several non-invasive sensors placed at the IV therapy site that can monitor the changes in the local physiology of the tissue and skin have been investigated in the literature toward detection of the leakage of fluid into the extravascular space. Fluidic resistance was tested to detect IV infiltration in [7]. In [8], an optical sensor-based system was used to detect IV infiltration. The sensing methods investigated in this proof-of-concept work are electrical bioimpedance (EBI) (to quantify local edema at IV site), and skin strain (to quantify the swelling of the skin as fluid accumulates locally at the IV site). The reasons for selecting these sensing methods were that local edema and skin swelling at the IV site due to escaping fluid into the extravascular space are two hallmark signs of IV infiltration [1], and both EBI and strain measurements could readily be achieved using low-power, inexpensive, and miniaturized hardware [9]–[14]. The goal is the detection of the escaping fluid into the extravascular space with low false alarm rates. In [15], preliminary results on EBI and skin strain sensing for fluid injection into an *ex vivo* tissue specimen were presented, where the focus was development of an embedded instrumentation system rather than biological testing and validation. This paper uses the pig model to further validate, in a proof of concept laboratory setting, the idea of using these sensing modalities for detecting an IV infiltration.

The study described in this paper investigates in an animal model the concept of using non-invasive, peripheral physiological sensing to detect an IV infiltration event. The main objective of this study is to perform proof-of-concept experiments in a controlled laboratory setting using a pig model to assess the feasibility of using EBI and skin strain modalities for detecting IV infiltration. This will then serve as an important step toward translation of non-invasive IV infiltration detection technologies to clinical use, which would ultimately improve patient safety.

II. METHODS AND PROCEDURES

A. SENSING AND INSTRUMENTATION SYSTEM

We focused on the evaluation of non-invasive and inexpensive sensing modalities to detect an IV infiltration. The sensing and instrumentation system were designed to detect the local fluid accumulation under the skin due to an IV infiltration. The measurement hardware used for sensing EBI and skin strain are described below.

1) ELECTRICAL BIOIMPEDANCE

Fluid leakage into the tissue can potentially be sensed by measuring the changes in EBI around the IV catheter site. Localized accumulation of the IV fluids would change the measured impedance across the IV site [15]–[17]. The EBI measurement comprises the injection of a small, safe, alternating electrical current to measure the voltage drop across the electrodes placed on the body. EBI was measured in this study using Ag/AgCl wet electrodes in a tetrapolar configuration [15]: four electrodes placed symmetrically across the IV site (outer two electrodes for current excitation, and inner two electrodes for voltage sensing). We employed the EBI100C amplifier (Biopac Systems Inc., Goleta, CA). The frequency of the injected 400μA (rms) sinusoidal current was set to 100kHz [17]–[19]. Bioresistance and bioreactance were derived using the magnitude and phase of the EBI, which were obtained from the EBI100C module. The studies were designed to determine whether the changes in EBI associated with small leakage of fluid ($<$5 mL) into the surrounding tissue would be detectable by the future wearable EBI hardware designs based on our group's prior work [9], [10], [15].

2) SKIN STRAIN

The fluid leaking into the tissue causes local skin deformation, i.e., stretching and even swelling in case of prolonged fluid accumulation. The local stretch and swelling of the skin due to infiltration can potentially be sensed as strain around the IV catheter. Therefore, to sense the skin deformation, we developed a skin strain sensor based on a silicone-coated strain gauge. The silicone coating has two purposes: protecting the sensor from any moisture intake, and extending the sensing area.

We used the KFH-6-120-C1-11L1M2R strain gauge (Omega Engineering Inc., Norwalk, CT) as shown in Fig. 1(a), with a nominal resistance of 120Ω. This strain gauge was selected because of its small size and high sensitivity. The mold for silicone coating of the strain gage is shown in Fig. 1(b), which was made by utilizing a 3D printer (LulzBot TAZ 5, Aleph Objects Inc., Loveland, CO). The dimensions of the mold were as follows: 18mm$\times$18mm upper square connected to a lower rectangle 10mm$\times$25mm through a 4mm width path, and depth of 0.75mm. For the silicone coating, room-temperature vulcanizing silicone rubber was used. Silicone rubber was poured in after the strain gage was placed in the mold, and then approximately one day of drying time was required. The silicone-coated skin strain sensor is shown in Fig. 1(c). Skin strain signals were pre-amplified using a custom analog front-end (see Fig. 2) consisting of a Wheatstone bridge with 120Ω resistors (the skin strain sensor is connected as a leg of the bridge), an instrumentation amplifier, a low pass filter (cutoff frequency = 3.3Hz), and a 5V regulator for single supply powering.

IEEE Journal of Translational Engineering in Health and Medicine

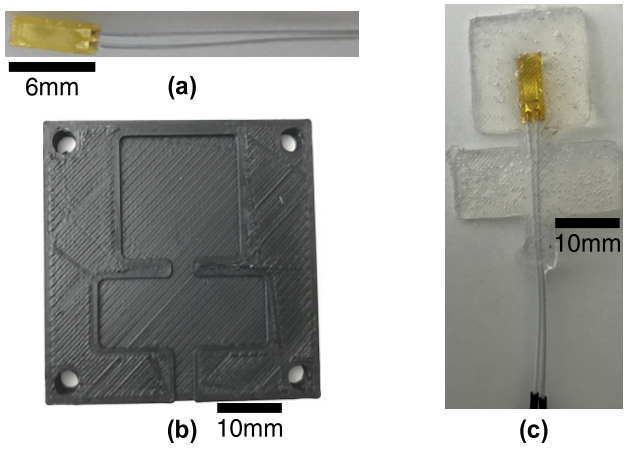

FIGURE 1. **Strain gage (a), mold for silicone coating (b), skin strain sensor made of silicone-coated strain gage (c).**

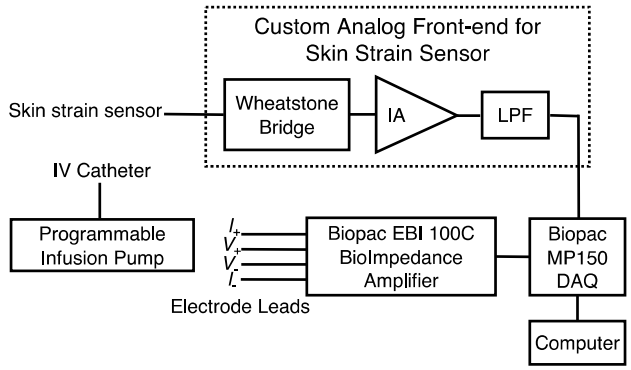

FIGURE 2. **Block diagram representation of the instrumentation and the data acquisition system. Custom analog front-end for skin strain sensing is composed of Wheatstone bridge, instrumentation amplifier (IA), and low pass filtering (LPF) blocks. I_+ and I_- are the leads for current excitation, V_+ and V_- are the leads for voltage sensing of the bioimpedance amplifier.**

3) SIGNAL ACQUISITION AND PRE-PROCESSING

The sensing elements were connected to an MP150 data acquisition (DAQ) system (Biopac Systems Inc., Goleta, CA). The sampling rate was set to 1kHz. The overall block diagram of the instrumentation and DAQ is shown in Fig. 2.

Considering the slow fluid infusion rates in IV injection (approximately 0.05mL/sec [20]), consequential changes in the sensor response are not expected in sub-second time-scale. Therefore, a 1000-point moving average filter was applied to the signals (each signal point in the measured response was averaged combining the points up to 0.5sec before and after) for smoothing. For the computation of decision variable x during real-time monitoring, the moving average can be implemented by introducing a processing delay of 0.5sec.

The decision variable, x, was normalized based on relative absolute difference of the sensor response, s, as

$$x_{m,n}^{(p,q)} = \frac{\left|s_{m,n}^{(p,q)}\left(t=T_{m,n}^{(q,\text{start})}\right)-s_{m,n}^{(p,q)}(t=T_{m,n}^{(q,\text{end})})+\tau_{\text{wait}}\right|}{s_{m,n}^{(p,q)}\left(t=T_{m,n}^{(q,\text{start})}\right)}, \tag{1}$$

where m is the experiment index, n is the vein infusion or IV infiltration indicator ($n = 0$ for infusion into vein, $n = 1$ for IV infiltration), p is the sensing modality index ($p = 1$ for bioresistance, $p = 2$ for bioreactance, $p = 3$ for skin strain), q is the infusion volume index ($q = 1$ for 2mL, $q = 2$ for 5mL, $q = 3$ for 10mL, $q = 4$ for the second 10mL), and $T_{m,n}^{(q,\text{start})}$ is the instant when the infusion of the qth volume starts, $T_{m,n}^{(q,\text{end})}$ is when the infusion of qth volume ends. A waiting duration of $\tau_{\text{wait}} = 4$min was introduced for the calculation of the relative absolute difference after the completion of an infusion volume (for the baseline recording).

B. ANIMAL EXPERIMENTS

We designed a study involving a large animal model (pigs) to determine the sensing requirements, both in terms of modalities and sensing specifications, for IV infiltration detection. A total of three animals were tested for IV infusion of 0.9% saline solution in the distal aspect of the lateral saphenous vein, and five animals were tested for infiltration of the saline solution in the surrounding tissue of the same vein segment. Because the variability in sensor data in response to the infusion of fluid directly into the vein was very low (see results below), only three animals were required for the control data (infusion into vein). The decision variable in (1) addresses the animal variability by assessing the changes in the EBI and strain measurements with respect to their corresponding baseline values. In the following paragraphs, the location of the sensors and the experimental protocol are described.

1) SENSOR PLACEMENT

Animals were under anesthesia for all experiments. The hind limb was shaven, the skin was disinfected with alcohol, and the IV catheter was placed before attaching the sensors. The location of the sensors is shown in Fig. 3. The electrodes used for EBI sensing were placed symmetrically in the proximity of the IV catheter site (two proximally to the site, and two distally). Placement of electrodes in the tetrapolar configuration on a hind limb of a pig is illustrated in Fig. 3. The electrodes were fixated to the skin by taping to ensure good contact was preserved throughout the experiment.

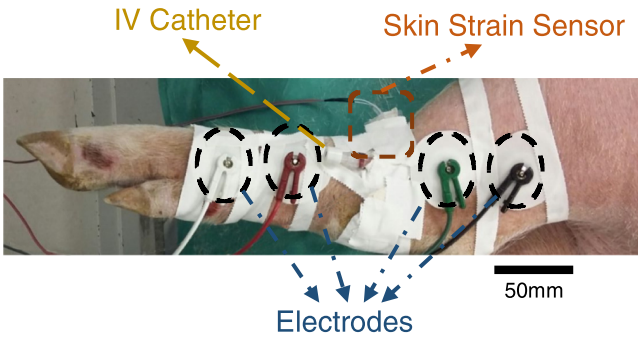

FIGURE 3. **Sensor placement on a hind limb of an anesthetized pig.**

Strain was measured using the developed skin strain sensor, which is sensitive to the local strain due to swelling of the skin. The skin strain sensor was placed next to the tip of the

IV catheter for both infusion into the vein and IV infiltration cases, and fixated using tape.

2) PROTOCOL

All animal testing procedures and protocols were approved by the T3 Labs and Georgia Tech Institutional Animal Care and Use Committee (IACUC). Each animal was under general anesthesia throughout the experiments. Experiments were composed of two separate parts for IV infusion (Part A) and infiltration (Part B). The PHD2000 (Harvard Apparatus, Holliston, MA) was used as the programmable infusion pump for both Part A and Part B. The fluid volumes of 2mL, 5mL, and 10mL were selected based on consultation with our clinical collaborators at Children's Healthcare of Atlanta. Detection of an IV infiltration with a resolution of less than 5 mL would represent a major advancement in clinical safety. Cases with serious injury typically have infiltration volumes of tens of mL of fluid. The injection rate was set to 2mL/min. A 20-gauge IV catheter was placed in the lateral saphenous vein of the anesthetized pig. The steps of the experimental procedure are explained in the following.

Part A—IV Infusion:

1) The IV catheter was positioned in the vein, and the physiological saline solution was administered to test the parameters under a normal IV Infusion.
2) A 5min baseline measurement was taken before infusion of the fluid starts.
3) Four fluid volumes were delivered using the infusion pump with a rate of 2mL/min in the following increments: 2mL, 5mL, 10mL, and the second 10mL (the total volume of the delivered fluid is 27mL). There was a 4min delay after the completion of each volume of infusion.
4) Following the final infusion of the second 10mL, a 10min delay was introduced for a final measurement.

Part B — Infiltration:

1) The catheter was repositioned by directing the tip of the catheter outside the vein into the surrounding subcutaneous tissue to physically simulate the IV infiltration.
2) Part A.2 was repeated.
3) Part A.3 was repeated.
4) Part A.4 was repeated.

C. STATISTICAL DISTINGUISHABILITY AND HYPOTHESIS TESTING

The overall IV infiltration detection strategy is illustrated in Fig. 4. We performed two sets of studies. First, we studied the distinguishability of the IV infiltration and the vein infusion. Second, we evaluated the ability to detect an infiltration with basic algorithms, including approaches that fuse both modalities.

For evaluating distinguishability, we used decision variable statistics (mean and standard deviation), and unpaired Student's t-test [21]. A p-value of less than 0.05 was considered statistically significant.

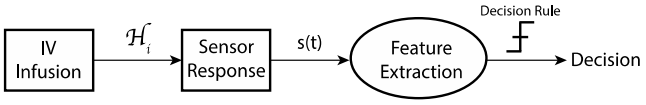

FIGURE 4. Block diagram representation of the IV infiltration detection system. H_i is the event ($i = 0$ for vein infusion, $i = 1$ for IV infiltration), and s is the measured sensor response.

For the hypothesis testing, we studied the decision problem on whether an IV infiltration event has occurred ($\mathcal{H}_1$) or not ($\mathcal{H}_0$, vein infusion). The variable μ_i corresponds to the mean of the decision variable x for a sensing modality for each event $\mathcal{H}_i$, and λ is the decision threshold for the corresponding sensing modality. We should note that x is calculated using the normalization given in (1). The decision variable, x, is compared to the corresponding threshold, λ, to decide on $\mathcal{H}_0$ or $\mathcal{H}_1$ (see Fig. 4).

The variable x given $\mathcal{H}_i$ has an experimentally specified different mean μ_i for each sensing modality and infused fluid volume. We assume the decision variable x for each sensing modality is normally distributed as $p(x|\mathcal{H}_i) \sim \mathcal{N}(\mu_i, \sigma_i^2)$, where σ_i^2 is the experimentally specified variance of x given $\mathcal{H}_i$.

Formulation of the probability of false alarm, i.e., false positive, and detection is as follows [22]. The probability of false alarm is obtained using the distribution of decision variable x given $\mathcal{H}_0$ as

$$P_f = p(x > \lambda|\mathcal{H}_0) = \int_\lambda^\infty p(x|\mathcal{H}_0) \tag{2}$$

Similarly, the probability of detection, i.e., true positive, is obtained using the distribution of decision variable x given H_1 as

$$P_d = p(x > \lambda|\mathcal{H}_1) = \int_\lambda^\infty p(x|\mathcal{H}_1) \tag{3}$$

To obtain the ROC curves, first λ value of each sensing modality was calculated by taking inverse of (2) at each P_f. Then, based on (3), P_d values were computed using corresponding λ values for each P_f. This was repeated for all sensing modalities at all fluid volumes.

D. SENSOR FUSION

Sensor fusion was studied based on the binary detection results of the individual sensors. Performance of three different fusion rules were investigated: 1) logical AND rule, 2) logical OR rule, and 3) majority rule (more than half of the sensors' decisions are positive or negative). To evaluate the sensor fusion performance, an operating point, i.e., a pair of P_d and P_f, on the ROC curve of each sensing modality was selected. The selection of the operating point was performed on the basis of minimizing P_f while maximizing the P_d for individual sensors. Using the selected operating point (P_d and P_f pair), binary detection results were generated for each sensing modality using a random number generator, and fusion rules were applied. Sensor fusion simulations were repeated 1000 times. Then, successful detection and false alarm rates were calculated for each fusion rule.

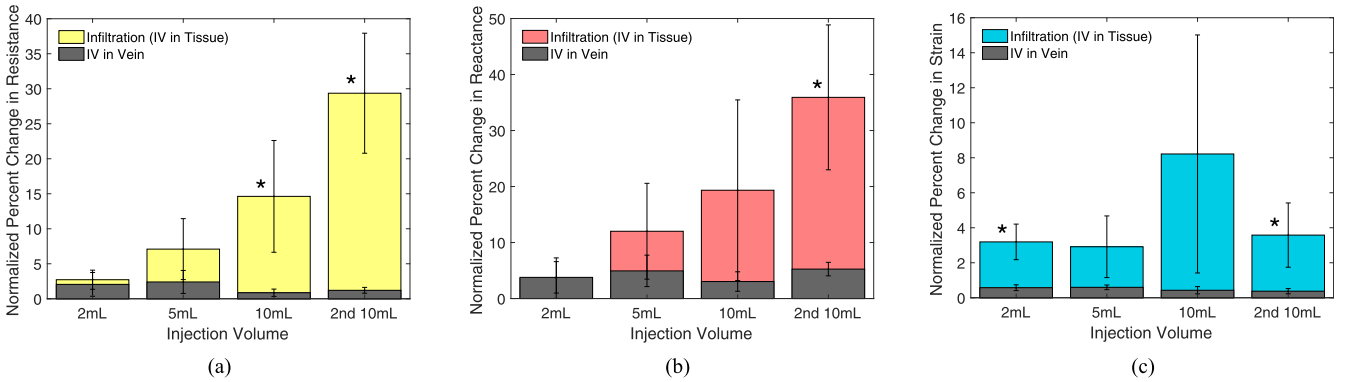

FIGURE 5. Comparison of the sensing modalities with respect to the volume of infusion (bioresistance (a), bioreactance (b), and skin strain (c)). Sensor responses were given for both vein infusion (grey bars) and infiltration (colored bars) cases. Changes in the sensors' responses are shown for an infiltration event (sensor responses were normalized using (1) and converted to percentage values). Input volumes of 2mL, 5mL, 10mL, and the second 10mL were used. Asterisk (∗) on the bar plots indicates $p < 0.05$ for the corresponding fluid volume. Based on animal-specific responses for bioresistance, bioreactance, and strain during infiltration, measurements from different animals gave a range of values. This may reflect the fat ratio in the limb, firmness of the limb skin, and sensor responses take a range of values based on each animal's individual response to infiltration.

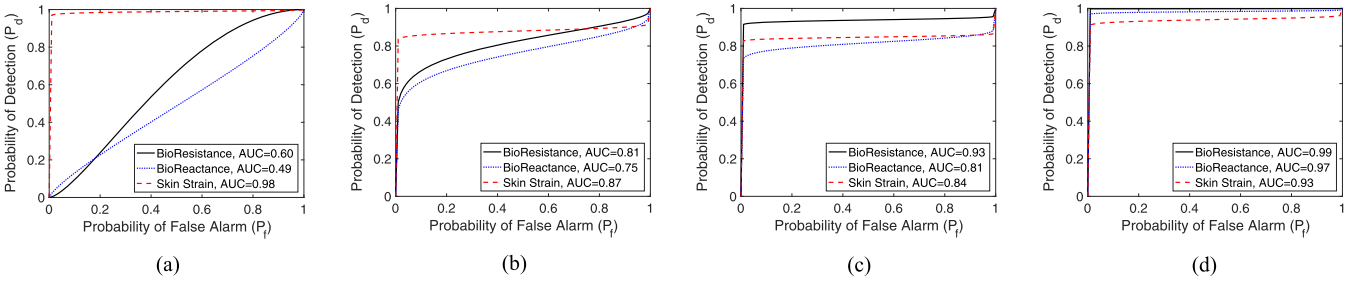

FIGURE 6. Receiver operating characteristics (ROC) curves (the false alarm probability (P_f) versus the detection probability (P_d)) for fluid volumes of 2mL (a), 5mL (b), 10mL (c), and second 10mL (d). ROC curves show the trade-off between probability of detection and false alarm for each sensing modality. When selecting the decision threshold λ, ROC curves need to be used to select the operating point according to constraints on P_d and P_f (false alarms would waste the resources including the medical professional's time, while missing events would be a safety concern). P_d higher than a given design constraint is desirable, while P_f is lower than a given design constraint is preferred. ($P_d = 1$ and $P_f = 0$ would be the desired operating point). Area under curve (AUC) is given in the legend for each sensing modality (AUC = 1 is the best case).

III. RESULTS

A. STATISTICAL DISTINGUISHABILITY

In Fig. 5(a), (b), and (c), mean bioresistance, bioreactance, and skin strain responses are shown with bar plots, respectively. The error bars correspond to the standard deviation. Changes in bioresistance and bioreactance responses increase with the increasing infused fluid volume. However, both bioresistance and bioreactance sensing have a lower change in the response level for vein infusion versus the IV infiltration at 2mL infusion compared to the skin strain sensing. An asterisk (∗) is used to indicate statistical significance. The skin strain sensor performed better for the detection of IV infiltration when the leaking fluid volume was only 2mL.

B. HYPOTHESIS TESTING

1) DETECTION PERFORMANCE FOR CONSTANT FALSE ALARM RATE

Here, we give the detection probabilities for a constant false alarm probability of 0.05. The decision threshold, λ, is adjusted for each case to satisfy the constraint on the probability of false alarm $P_f = 0.05$ based on the decision variable statistics of the corresponding sensing modality given H_0. The detection probabilities for each case are calculated using the decision variable statistics given H_1 for the corresponding sensing modality.

The detection probability of bioresistance sensing for the 10mL case is greater than 0.9. The IV infiltration detection probabilities for both bioresistance and bioreactance are greater than 0.9 for the second 10mL case. The detection probabilities of skin strain sensing for the 2mL and second 10mL cases are greater than 0.9.

In addition, for the 10mL cases, bioreactance sensing has detection probability greater than 0.7. Skin strain sensing has detection probabilities greater than 0.8 for the 5mL and 10mL cases.

2) FALSE POSITIVE (P_f) *VS TRUE POSITIVE* (P_d)

Receiver operating characteristic (ROC) curves are given in Fig. 6 for 2mL, 5mL, 10mL, and second 10mL cases. ROC curves give the trade-off between the false alarm and detection probabilities. While a decreased threshold level, λ,

TABLE 1. Selected operating points for individual sensors and sensor fusion results (bolo entries are for $P_d > 0.85$ and $P_f < 0.05$).

		2mL		5mL		10mL		Second 10mL	
		P_d	P_f	P_d	P_f	P_d	P_f	P_d	P_f
Sensing Modality	BioResistance	0.5	0.67	0.66	0.09	**0.91**	**0.01**	**0.99**	**0.01**
	BioReactance	0.52	0.5	0.6	0.09	0.73	0.01	**0.97**	**0.01**
	Skin Strain	**0.97**	**0.010**	0.83	0.01	0.82	0.01	**0.91**	**0.01**
Fusion Rule	Logical OR	0.99	0.67	0.97	0.096	**0.99**	**0.019**	**0.99**	**0.021**
	Logical AND	0.25	0.0061	0.33	0.0008	0.54	0.0001	**0.88**	**0.0003**
	Majority Rule	0.74	0.67	0.79	0.086	**0.92**	**0.0087**	**0.997**	**0.011**

can provide better detection probability, false alarm (false positive) probability may also be increased. Furthermore, the larger the area under the curve (AUC), the higher the accuracy of the sensing modality for detection of IV infiltration at the corresponding leaking fluid volume.

For the detection of small leaking fluid volumes of 2mL and 5mL in Fig. 6(a) and (b), skin strain sensing achieves better classification performance compared to the sensing modalities based on EBI, i.e., bioresistance and bioreactance. As the amount of leaking fluid volume increases, e.g., 10mL and second 10mL cases, detection of IV infiltration using bioresistance sensing is observed to be providing better detection accuracy in Fig. 6(c) and (d) for a given false alarm constraint.

3) FUSION OF SENSING MODALITIES

For the 2mL, 5mL, 10mL, and second 10mL fluid volumes, the selected operating point for individual sensors and sensor fusion results are tabulated in Table I. The logical OR rule has an impact of increasing the detection rate, P_d, at the expense of increasing the false alarm rate with respect to the performance of individual sensing modalities. The logical AND rule decreases the false alarm rate, P_f, however, the detection rate, P_d, is also reduced. Sensor fusion can help to further improve the performance of individual sensors, as well as to compensate for the low performance of individual sensors at lower or higher fluid volumes.

C. DISCUSSION

The characterization of the non-invasive sensing modalities undertaken provides an understanding of the performance and ranges that are associated with the detection of IV infiltration. The EBI and skin strain modalities are utilized to distinguish between vein infusion and IV infiltration based on the animal studies. IV infiltration can be detected in a real-time manner by fusing the multiple sensing modalities. While location of the skin strain sensor is more susceptible to positional errors, it provides a more accurate detection performance for lower fluid volume injection than the bioresistance and bioreactance sensing modalities.

For the optimization of the decision threshold, the costs associated with the false alarms and misdetections need to be further elaborated. Higher false alarm rates may consume more of the caregivers' time, and ultimately lead to the alarms being ignored due to being unreliable. When the infused fluid is especially harmful to skin, veins, and tissue, decision thresholds for the sensors can be adjusted to detect an IV infiltration as quickly as possible, so that, the patient can be protected at the expense of increased false alarm rates.

Bioimpedance and bioreactance may exhibit variations in the baseline responses due to subject-specific anatomical differences including body water volume. Skin strain may also show variations in response to an IV infiltration event due to subject-specific skin elasticity. Therefore, the developed detection algorithms in the future for the detection of IV infiltration should be adaptive to the subject-specific statistics of the sensor responses.

The EBI and skin strain measurements would be corrupted by noise due to the movement of the body as well as the attaching position of the sensors. Addition of redundant sensors as well as a motion sensor could help to address this challenge. The standardization of the positioning of sensors will require extensive field testing. The issues of motion artifacts and optimal sensor positioning are left as future work. The performance evaluations presented in this paper constitute a proof-of-concept and provide a comparison of sensing modalities, which can be used by researchers as a foundation for designing wearable devices for this application.

The hardware systems for EBI and skin strain sensing in this proof-of-concept work are relatively expensive due to the need for bench-top instrumentation for data collection. A customized wearable version of the hardware could decrease the overall cost of the system and could fit directly onto the patient's arm at the IV site to reduce the hindrance for an already cluttered bedside.

IV. CONCLUSION

This paper provides a performance evaluation of non-invasive sensing of EBI and skin strain sensing around the IV catheter site as proof-of-concept for the automated detection IV infiltration. Statistical comparisons are performed based on the experimental data collected using animal experiments for bioresistance, bioreactance, and skin strain sensing modalities. The sensing modalities were tested on a hind limb of

anesthetized pig by physically simulating IV infiltration. The results show that the EBI and skin strain sensing modalities can be used to reliably detect IV infiltration under controlled laboratory conditions, where movement of the subject and related noise factors are not considered. Future work includes the development of a miniaturized, low-cost and energy-efficient apparatus, as well as performing measurements on human subjects that are being administered IV therapy.

REFERENCES

[1] R. J. Kumar, S. P. Pegg, and R. M. Kimble, "Management of extravasation injuries," *ANZ J. Surg.*, vol. 71, no. 5, pp. 285–289, 2001.

[2] D. Camp-Sorell, "Developing extravasation protocols and monitoring outcomes," *J. Inf. Nursing*, vol. 21, no. 4, pp. 232–239, 1998.

[3] P. H. T. Cartlidge, P. E. Fox, and N. Rutler, "The scars of newborn intensive care," *Early Hum. Develop.*, vol. 21, no. 1, pp. 1–10, 1990.

[4] V. Paquette, R. McGloin, T. Northway, P. DeZorzi, A. Singh, and R. Carr, "Describing intravenous extravasation in children (DIVE study)," *Can. J. Hospital Pharmacy*, vol. 64, no. 5, pp. 340–345, Sep./Oct. 2011.

[5] A. J. Raimondi, *Pediatric Neurosurgery: Theoretical Principles-Art of Surgical Techniques*. Berlin, Germany: Springer-Verlag, 1998.

[6] C. E. Wilkins and A. J. B. Emmerson, "Extravasation injuries on regional neonatal units," *Arch. Diseases Childhood-Fetal Neonatal Ed.*, vol. 89, no. 3, pp. F274–F275, 2004.

[7] D. A. Scott *et al.*, "Detection of intravenous fluid extravasation using resistance measurements," *J. Clin. Monitor.*, vol. 12, no. 4, pp. 325–330, 1996.

[8] L. W. Winchester and N.-Y. Chou, "Optical detection of intravenous infiltration," in *Proc. SPIE*, vol. 6080. Feb. 2006, Art. no. 608016.

[9] S. Hersek, H. Töreyin, and O. T. Inan, "A robust system for longitudinal knee joint edema and blood flow assessment based on vector bioimpedance measurements," *IEEE Trans. Biomed. Circuits Syst.*, vol. 10, no. 3, pp. 545–555, Jun. 2016.

[10] S. Hersek *et al.*, "Wearable vector electrical bioimpedance system to assess knee joint health," *IEEE Trans. Biomed. Eng.*, vol. 64, no. 10, pp. 2353–2360, Oct. 2017.

[11] A. Hartov *et al.*, "A multichannel continuously selectable multifrequency electrical impedance spectroscopy measurement system," *IEEE Trans. Biomed. Eng.*, vol. 47, no. 1, pp. 49–58, Jan. 2000.

[12] J.-B. Chossat, Y.-L. Park, R. J. Wood, and V. Duchaine, "A soft strain sensor based on ionic and metal liquids," *IEEE Sensors J.*, vol. 13, no. 9, pp. 3405–3414, Sep. 2013.

[13] Y.-L. Park, B.-R. Chen, and R. J. Wood, "Design and fabrication of soft artificial skin using embedded microchannels and liquid conductors," *IEEE Sensors J.*, vol. 12, no. 8, pp. 2711–2718, Aug. 2012.

[14] A. Nag, S. C. Mukhopadhyay, and J. Kosel, "Wearable flexible sensors: A review," *IEEE Sensors J.*, vol. 17, no. 3, pp. 3949–3960, Jul. 2017.

[15] J. A. Jambulingam, R. McCrory, L. West, and O. T. Inan, "Non-invasive, multi-modal sensing of skin stretch and bioimpedance for detecting infiltration during intravenous therapy," in *Proc. IEEE EMBC*, Orlando, FL, USA, Aug. 2016, pp. 4755–4758.

[16] J. G. Webster, *Encyclopedia of Medical Devices and Instrumentation*, 2nd ed. Hoboken, NJ, USA: Wiley, 2006.

[17] J.-H. Kim, B.-J. Shin, S.-W. Baik, and G.-R. Jeon, "Early detection of intravenous infiltration using multi-frequency bioelectrical impedance parameters: Pilot study," *J. Sensor Sci. Technol.*, vol. 26, no. 1, pp. 15–23, 2017.

[18] H. Cao, S. Tungjitkusolmun, Y. B. Choy, J. Z. Tsai, V. R. Vorperian, and J. G. Webster, "Using electrical impedance to predict catheter-endocardial contact during RF cardiac ablation," *IEEE Trans. Biomed. Eng.*, vol. 49, no. 3, pp. 247–253, Mar. 2002.

[19] H. Kalvoy, L. Frich, S. Grimnes, O. G. Martinsen, P. K. Hol, and A. Stubhaug, "Impedance-based tissue discrimination for needle guidance," *Physiol. Meas.*, vol. 30, no. 2, pp. 129–140, 2009.

[20] L. Caroll, *Acute Medicine: A Handbook for Nurse Practitioners*. West Sussex, U.K.: Wiley, 2007.

[21] J. H. McDonald, *Handbook of Biological Statistics*, 3rd ed. Baltimore, MD, USA: Sparky House Publishing, 2014.

[22] H. L. Van Trees, *Detection, Estimation, and Modulation Theory, Part I: Detection, Estimation, and Linear Modulation Theory*. New York, NY, USA: Wiley, 1968.